IOP Publishing Journal of Physics: Condensed Matter
J. Phys.: Condens. Matter **32** (2020) 175501 (7pp) https://doi.org/10.1088/1361-648X/ab6a30

Electronic structures of 24-valence-electron full Heusler compounds investigated by density functional and *GW* calculations

Hung-Wen Lee[1], Cheng-Rong Hsing[1], Chun-Ming Chang[2] and Ching-Ming Wei[1,3]

[1] Institute of Atomic and Molecular Sciences, Academia Sinica, Taipei 10617, Taiwan, Republic of China
[2] Department of Physics, National Dong Hwa University, Hualien 97401, Taiwan, Republic of China
[3] Institute of Physics, Academia Sinica, Nankang 11529, Taiwan, Republic of China

E-mail: cmc@mail.ndhu.edu.tw and cmw@phys.sinica.edu.tw

Received 22 October 2019, revised 3 December 2019
Accepted for publication 10 January 2020
Published 28 January 2020

Abstract

The electronic structures of Fe-based and Ru-based full Heusler compounds have been investigated systematically by density functional theory (DFT) with PBE, PBE + U, and HSE06 exchange-correlation (XC) functionals. In order to have a better systematic and quantitative comparison between the results of different approximations, the average deviation of eigenvalues (ADE) between any two electronic band structures were calculated. From quantitative analysis of the ADEs, we have shown that different XC functionals used in the DFT calculations will result in very different and inconsistent electronic band structures. However, the discrepancies are dramatically reduced and get more consistent band structures after the *GW* calculations. Furthermore, comparing the experimental and calculated Seebeck coefficients and band-gap values of Fe_2VAl, it implies that the *GW* methods including dynamically screened Coulomb interactions are more reliable than DFT with PBE or HSE06 functionals. Conclusively, contrast to the fact that DFT methods give inconsistent band structures when using different XC functionals, the *GW* methods have better predictive power for the band structures of Fe-based and Ru-based full Heusler compounds.

Keywords: density functional theory, *GW* approximation, Heusler compound, band structure, Seebeck coefficient

S Supplementary material for this article is available online

(Some figures may appear in colour only in the online journal)

Introduction

Thermoelectric materials can convert waste heat to electricity and thus play an important role in the field of renewable energy generation [1]. Among the various types of thermoelectric materials, Heusler compounds are found to have potential applications in this field [2]. The efficiency of thermoelectric materials can be measured quantitatively by the figure of merit $ZT = (S^2\sigma T)/(\kappa_l + \kappa_e)$, where S, σ, κ_l, and κ_e are the Seebeck coefficient, electrical conductivity, lattice thermal conductivity, and electrical thermal conductivity, respectively. These transport properties strongly depend on the electronic structures of the materials. Therefore, accurate electronic structures are essential for theoretical prediction of the efficiency of thermoelectric materials.

First-principles density functional theory (DFT) [3, 4] is the most popular method for the theoretical calculations of electronic structures of solid systems, and has been applied extensively to study the thermoelectric properties of Heusler compounds [5–8]. However, there is a limitation for Kohn–Sham (KS) DFT to predict accurate band structures as the KS single-particle eigenvalues are not meant to resemble the

actual excitations. For the exact KS theory, without hybrids, does predict the band gap correctly if the derivative discontinuity of the exchange-correlation (XC) functional is taken into account [9, 10]. Thus the exact KS DFT and exact quasiparticle theory equal on at two points on a semiconductor. However, they differ by additional quasiparticle shifts, as KS eigenvalues are only zeroth order approximations to electron removal and addition energies. Thus this would restrict the reliability of the derived thermoelectric properties. For example, the electronic structures of Fe_2VAl obtained by various XC functionals are highly controversial, and their predicted properties varied from semimetal [11–13] to semiconductor [5, 6]. Unfortunately, this controversy could not be resolved even when comparing with the experimental results. From nuclear magnetic resonance (NMR) and optical conductivity experiments, inter-band transitions of 0.21–0.28 [14] and 0.10 eV [15] were measured, respectively. However, without the angle resolved photoemission spectroscopy (ARPES) experimental data, it is difficult to recognize the transition is due to a real band gap that corresponding to a semiconductor, or a pseudogap that corresponding to a semimetal. Furthermore, Bilc *et al* have used hybrid functional to calculate the thermoelectric power factor of Fe-based Heusler compounds (Fe_2YZ) and claimed that all of them are intrinsic semiconductors [5]. However, oppositely some of them have been predicted to be semimetals or narrow-band-gap semiconductors by using local or semilocal functionals [11, 12, 16, 17]. Therefore, a more accurate method beyond the DFT level is required from either fundamental predictions or practical applications.

The *GW* approximation [18, 19], which includes the many-body interactions by calculating the Green's functions (G) and dynamically screened Coulomb interaction (W), is to date the state-of-the-art method for electronic structure calculations, and has shown its ability to produce reliable band structures of semiconductors that can be meaningfully compared with experiments [20–23]. In contrast to the zeroth order DFT approximation, the XC potential in *GW* calculation is replaced by the many-body self-energy. *GW* studies for the bulk copper [24] and gold [25] have shown that the many-body corrections are crucial to reduce the discrepancies between DFT and experimental band structures. Moreover, there have been G_0W_0 studies for the half-metallic Co_2MnSi and Co_2FeSi full Heusler compounds [26] and almost-gapless (XX')YZ quaternary Heusler semiconductors [27]. These studies have pointed out that Perdew–Burke–Ernzerhof (PBE) [28] XC functional provided a reasonable approximation for the band structures [26, 27] and G_0W_0 with PBE starting wavefunctions can give advanced improvement; furthermore, PBE0 [29, 30] hybrid XC functional predict worse results than the PBE XC functional [26].

In our previous study that collaborated with experimental groups for the Ru_2NbGa [31] full Heusler compounds has shown that, the band structures calculated by the generalized gradient approximation of PBE and the hybrid HSE06 [32, 33] XC functionals within the DFT level are quite different (a semimetal for PBE and a semiconductor for HSE06). However, the difference between the band structures of two functionals is dramatically diminished and the band gap becomes very consistent after the many-body *GW* correction, and more importantly the results consist with experimental observations [31]. Similar behavior for the Ru_2TaAl [34] full Heusler compounds has also been observed recently. It is evident that *GW* calculations could remedy the inconsistency of band structures that obtained at DFT level.

Table 1. Comparison of the calculated (PBE) and experimental (EXP) lattice constants (a_0, with unit of Å.). The deviation is defined as: (a_0(PBE)—a_0(EXP))/a_0(EXP).

	a_0(PBE)	a_0(EXP)	Deviation (%)
Fe_2VAl	5.71	5.760 [14]	−0.9
		5.775 [50]	−1.1
Fe_2VGa	5.73	5.770 [51]	−0.7
Fe_2NbAl	5.92	N/A	
Fe_2NbGa	5.93	N/A	
Ru_2VAl	6.00	5.972 [52]	0.5
		5.980 [53]	0.3
Ru_2VGa	6.02	5.983 [52]	0.6
		5.994 [53]	0.4
Ru_2NbAl	6.19	6.135 [54]	0.9
Ru_2NbGa	6.20	6.150 [31]	0.8

In this paper, the electronic structures of the Fe-based and Ru-based non-magnetic full Heusler (X_2YZ) compounds (which obeying Slater-Pauling rule with 24 valence electrons in a unit cell) [35] will be studied systematically. As inspired by our previous studies on metallic clusters [36], the differences of electronic band structures between various approximation methods are systematically and quantitatively analyzed by calculating their average deviation of eigenvalues (ADE). We will show that, for all the Heusler compounds studied in this paper, although the electronic structures obtained at the DFT level with PBE, PBE + U, and HSE06 XC functionals are quite different, they became very similar and consistent at the *GW* level. Furthermore, taking Fe_2VAl as a demonstrating example, we will show that not only the band gap but also the Seebeck coefficients predicted at the GW_0 level for both PBE and HSE06 functionals are more consistent with experiments which indicating its correctness and accuracy with predictive power. These results strongly suggest that the *GW* many-body corrections are highly required to obtain the correct band structures of full Heusler compounds, and furthermore to predict their thermoelectric properties and efficiency.

Computational details

All DFT and *GW* calculations are performed using the Vienna *ab initio* simulation package (VASP) [37–41]. The interactions between the ions and valence electrons were described by the projected augmented wave (PAW) method [39, 42]. The KS equations were solved using the plane wave basis set with kinetic energy cutoff of 500 eV and 650 eV for Ru-based and Fe-based compounds, respectively. Both the PBE and HSE06 XC functionals have been used. The screened hybrid functional HSE06 contains 25% of short-range Hartree–Fock exact exchange, can yield realistic generalized KS gaps for

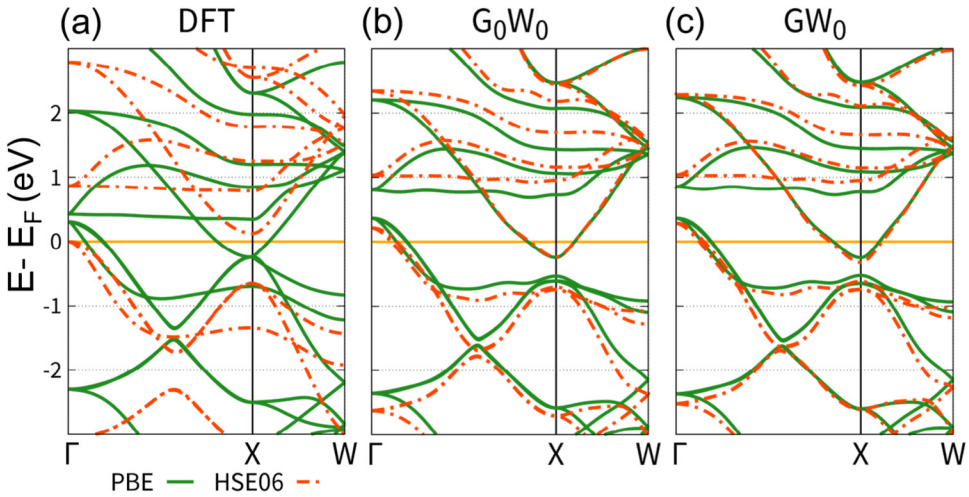

Figure 1. Comparison of the band structures calculated with the PBE and HSE06 XC functionals for Ru_2NbGa at (a) DFT, (b) G_0W_0, and (c) GW_0 levels.

typical semiconductors and also reduce the self-interaction error [43, 44]. For Fe-based compounds, the effect of Hubbard corrections (PBE + U [45] with $U_{Fe} = 2$ eV [7]) has also been investigated. The primitive cell of full Heusler alloy X_2YZ is of $L2_1$ structure. K-point sampling was constructed by a $(8 \times 8 \times 8)$ Γ-centered mesh [46]. All the lattice constants were obtained by fitting the energy-volume curves (using PBE functional) to the Murnaghan's [47] equation of state, and the results are shown and compared with experimental values in table 1. The electronic Green's function and the screened Coulomb potential for the non-self-consistent G_0W_0 and the partial self-consistent GW_0 calculations were constructed starting from DFT(KS) eigenfunctions and eigenvalues with PBE, PBE + U, and HSE06 functionals. Since an appreciable number of empty conduction bands is required for GW calculations, we have used total of 384 bands, which is ten times larger than the number of occupied bands. Band structures along the high symmetry directions were plotted from the Wannier band interpolation scheme using the wannier90 code [48, 49]. Through this paper, we use an abbreviation, methodology (XC functional), to represent the level of methodologies (DFT, G_0W_0, or GW_0), and the functional and/or starting wavefunction (PBE, PBE + U, or HSE06) used for a calculation. For instance, GW_0(HSE06) means that at GW_0 level, a HSE06 starting wavefunction is used and DFT(PBE) means at DFT level, PBE functional is used.

In order to have a detailed comparison of the electronic structures calculated by different approximations, the ADE is calculated to quantitatively determine the similarity of band structures between any two methods. First of all, the ADE for one specific k-point was defined as

$$\Delta^{\mathrm{KP}}_{\mathrm{M_1,\,M_2}} = \frac{\sum_n |E^{\mathrm{KP}}_{n,\mathrm{M_1}} - E^{\mathrm{KP}}_{n,\mathrm{M_2}}|}{N}, \tag{1}$$

where KP denotes a specific k-point, and $E^{\mathrm{KP}}_{n,\mathrm{M_1}}$ and $E^{\mathrm{KP}}_{n,\mathrm{M_2}}$ are eigenvalues of the nth band at the specific K-point calculated by the M_1 and M_2 methods. N is the total number of bands used to evaluate the average. Then, the ADE between the two approximations is the weighted sum of the deviation over the k-point set

$$\mathrm{ADE}_{\mathrm{M_1,\,M_2}} = \sum_{\mathrm{KP}} \omega_{\mathrm{KP}} * \Delta^{\mathrm{KP}}_{\mathrm{M_1,\,M_2}}, \tag{2}$$

where ω_{KP} is the weight of the corresponding irreducible k-point in the whole Brillouin zone.

Results and discussions

As mentioned in the Introduction section, the band structures for the Fe-based and Ru-based full Heusler compounds predicted by different XC functionals are quite controversial at the DFT level. Now, we take the Ru_2NbGa full Heusler compound as an example to demonstrate the discrepancy of the band structures between the PBE and HSE06 XC functionals at the DFT level, and the results are shown in figure 1(a). It is clear that these two band structures are not consistent with each other. While semimetallic behavior with a negative band gap (see definition below) of −0.545 eV is predicted by the DFT(PBE) calculations, a semiconductor with small gap of 0.130 eV is predicted by the DFT(HSE06) calculations. However, this discrepancy is dramatically diminished after the many-body GW correction has applied. The GW corrected band structures are shown in figure 1(b) for the G_0W_0 and figure 1(c) for the GW_0 approximations. Obviously, the dissimilarity at the DFT level is intensively reduced even at the non-self-consistent G_0W_0 level, and improved further at the partial self-consistent GW_0 level. The inconsistency of the electronic characteristics for DFT(PBE) (semimetal) and DFT(HSE06) (semiconductor) can be solved at the GW levels (both are semimetals for using PBE or HSE06 starting wavefunctions). The predicted pseudogaps of the semimetal within G_0W_0(PBE) and G_0W_0(HSE06) are −0.612 and −0.457 eV, and those with GW_0(PBE) and GW_0(HSE06) are −0.613 and −0.611 eV. It is interesting to note that, the semimetal characteristic has already been captured by DFT(PBE), while DFT(HSE06) has predicted the wrong characteristic

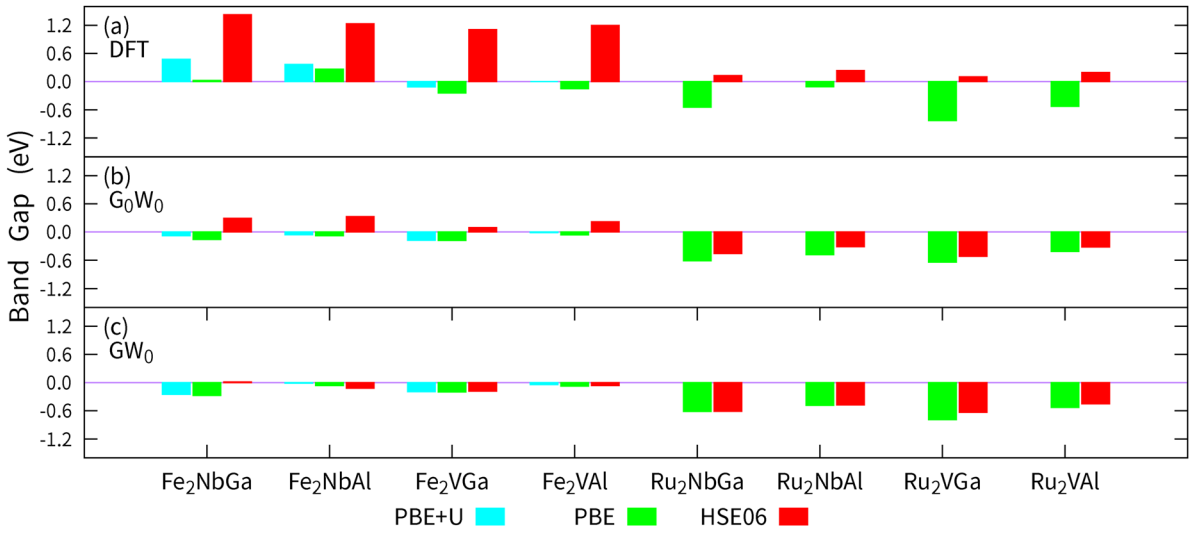

Figure 2. Comparison of the band gap calculated with the PBE, PBE + U (for Fe-based compounds only), and HSE06 XC functionals for the Heusler compounds at (a) DFT, (b) G_0W_0, and (c) GW_0 levels. The positive gaps correspond to the real gap with semiconductor characteristic. The negative gaps correspond to the pseudogap with semimetal/metal characteristic.

(semiconductor) as compared to the more consistent *GW* results. This phenomenon will be further investigated later in this section.

Starting from the Ru_2NbGa compound, we have systematically studied the Fe-based and Ru-based full Heusler compounds of X_2YZ (X = Fe, Ru; Y = V, Nb; Z = Al, Ga). The electronic structures for these Heusler compounds have been calculated at DFT and *GW* levels for both PBE and HSE06 functionals, and the results for the band gaps are summarized in figure 2. The band gap (E_g) is defined as $E_{N+1,\min}$ minus $E_{N,\max}$, where $N(=12)$ is half of the total number of valence electrons and $E_{N,\max}$ ($E_{N+1,\min}$) is the maximum (minimum) band energy of Nth ($(N+1)$th) band. Therefore, the overlap between the Nth and $(N+1)$th band for a semimetal will result in a negative band gap.

At the DFT level, the results obtained by DFT(PBE) and DFT(HSE06) are conflict with each other for most of the compounds as shown in figure 2(a). While most of the compounds are predicted to be semiconductors with real band gaps by DFT(HSE06), they are predicted to be semimetals/metals with negative band gaps by DFT(PBE). However, these controversial physical properties are obviously reduced at the G_0W_0 level as shown in figure 2(b); the electronic characteristic predicted by G_0W_0(PBE) and G_0W_0(HSE06) for Ru-based compounds became consistent with each other. Although the conflicts still exist for the Fe-based compounds at the G_0W_0 level, their differences are lessened when compared with the results at DFT level. At the GW_0 level, the discrepancies of the band gaps are largely diminished as shown in figure 2(c). Furthermore, both of GW_0(PBE) and GW_0(HSE06) predicted negative band gaps for all the Heusler compounds (except for the Fe_2NbGa, which has a very small band gap of 0.016 eV (nearly gapless) within GW_0(HSE06)), and the band gap values are also quite consistent with each other.

From figure 2, we can also observe the trend of the band gap characteristics predicted within one XC functional at different hierarchical levels. For HSE06, positive real band gaps are predicted for all the Fe-based and Ru-based Heusler compounds at DFT level, while half of them (for the Ru-based compounds) turn into semimetal/metal with negative band gaps at the G_0W_0 level, and all of them (except Fe_2NbGa) have negative band gaps at the GW_0 level. On the other side, for PBE, positive real band gaps for Fe_2NbGa and Fe_2NbAl compounds and negative band gaps for all the other compounds are predicted at the DFT level, while all of them have negative band gaps at both of the G_0W_0 and GW_0 levels. That is, using PBE functional can lead more consistent results between the DFT and *GW* levels than using HSE06 functional.

Although the DFT(PBE) has predicted band gaps similar to the GW_0(PBE) ones in most (6 out of 8) cases, there still exist some obvious discrepancies in band structures between them. Generally speaking, the accuracy of the calculated electronic structure could not be determined solely by the band gap. There is an obvious point, as shown in figure 1 for the band structure of Ru_2NbGa, it has no gap between the two states right below the Fermi level at the X point at the DFT level, while a gap of 0.28 eV is opened at the GW_0 level. Consequently, the ADE is calculated to systematically and quantitatively determine the similarity of the whole band structures between any two kinds of theoretical predictions.

The ADEs between PBE and HSE06 at the three different hierarchical levels for the Heusler compounds are shown in figure 3. The $ADE_{PBE,HSE06}$ for DFT level has the largest values (around 0.51–0.70 eV) among these three sets for all the materials. This phenomenon agrees with the contradiction of band gaps at DFT level as discussed above. Once the *GW* correction has been performed, the values of $ADE_{PBE,HSE06}$ drop instantly to around 0.14–0.35 eV. The small values of $ADE_{PBE,HSE06}$ for G_0W_0 and GW_0 levels imply the similarity of their corresponding band structures (for example, see the figures 1(b) and (c) for Ru_2NbGa). That is, the deviation of the band structures at DFT level for different XC functionals could be corrected by the *GW* calculations and thus result in comparable and reliable band structures.

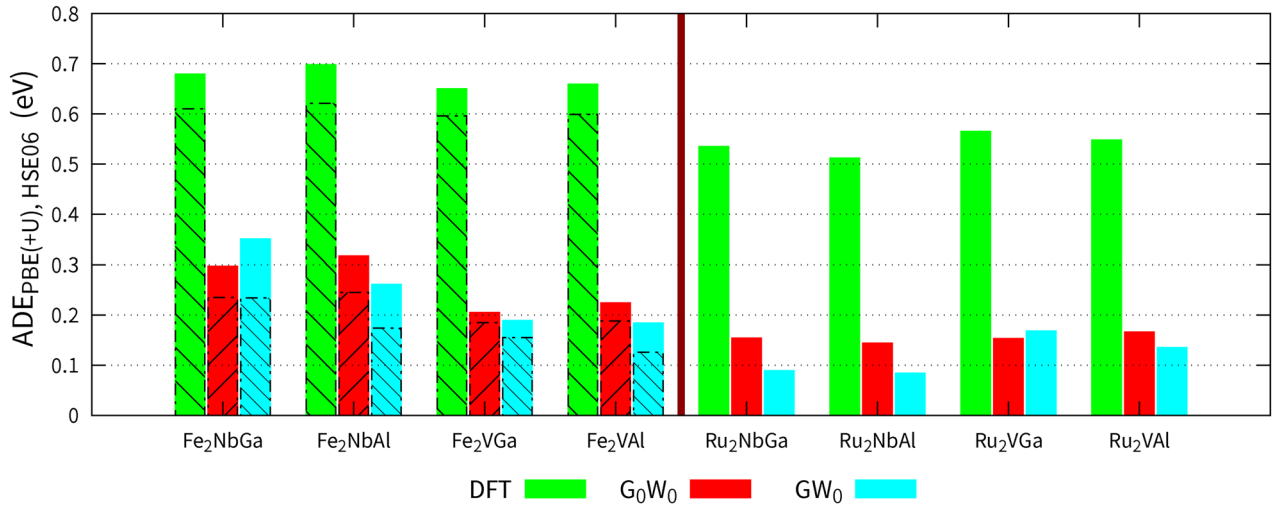

Figure 3. The ADEs between PBE and HSE06 exchange-correction functionals at DFT (green), G_0W_0 (red), and GW_0 (cyan) levels for the Heusler compounds. For the Fe-based compounds, the ADEs between the PBE + U (U_{Fe} = 2 eV) and HSE06 are shown as the dashed bar.

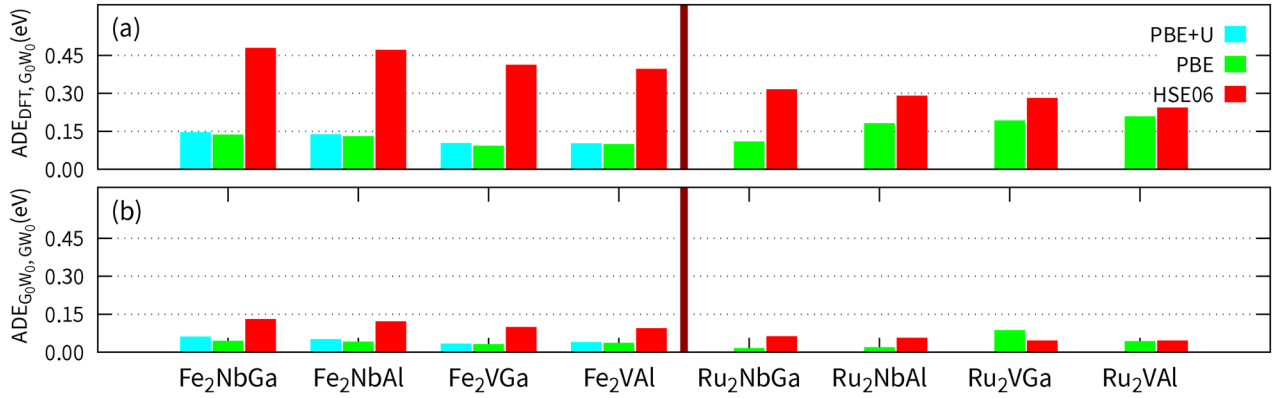

Figure 4. (a) The ADEs between DFT and G_0W_0 levels with the PBE, PBE + U (only for Fe-based compounds), and HSE06 XC functionals. (b) The ADEs between G_0W_0 and GW_0 levels with both PBE, PBE + U (only for Fe-based compounds), and HSE06 XC functionals.

Furthermore, to what extent the band structures being modified during the *GW* corrections could also be quantitatively analyzed by the ADE method, and the results are summarized in figure 4. Comparing the ADE$_{DFT,G_0W_0}$ for PBE and HSE06 in figure 4(a), it reveals that within the G_0W_0 approximation, the electronic structures of G_0W_0(HSE06) have been modified by a much larger proportion than those of G_0W_0(PBE) for most of the compounds. The small values of ADE$_{G_0W_0,GW_0}$ for PBE (less than 0.1 eV) shown in figure 4(b) indicate that, the main features of the band structures have arisen at the G_0W_0 level and thus have small improvement at GW_0 level. However, the ADE$_{G_0W_0,GW_0}$ for HSE06 are larger than those for PBE in most cases (especially for the Fe-based compounds). Combining the ADE results and discussions about the band gaps (figure 2), it reveals that merely G_0W_0(HSE06) is not enough to obtain converged results; further improvement by GW_0 correction is required for HSE06.

In addition, owing to the Hubbard corrections are usually added for the iron bearing materials in the DFT calculations, we have also performed the PBE + U (U_{Fe} = 2 eV) calculations for the Fe-based compounds. As expected, the Hubbard corrections have increased the band gaps (decrease the pseudogaps) at DFT level as shown in figure 2(a). After the GW_0 many-body corrections, the band-gap values obtained are quite consistent with each other as shown in figure 2(c) (except Fe$_2$NbGa which has a nearly zero gap for GW_0(HSE06)). Due to the increase of band gaps (decrease of pseudogaps) for PBE + U (as compared to the results of PBE), the ADE$_{PBE+U,HSE06}$ are smaller than ADE$_{PBE,HSE06}$ as shown in figure 3. Finally, the ADE$_{DFT,G_0W_0}$ and ADE$_{G_0W_0,GW_0}$ for PBE + U are similar to those for PBE, as shown in figure 4. This indicate that both PBE and PBE + U functionals have similar extent of modification by the *GW* corrections.

According to the current results and discussions, the more accurate and consistent band structures would be obtained after the G_0W_0 corrections for the PBE and PBE + U functionals (for Fe-based compounds), and GW_0 corrections for the HSE06 functional. Therefore, performing G_0W_0(PBE) calculations would be a good strategy to efficiently acquire the accurate band structures of these Heusler compounds.

Furthermore, as the electronic structures are essential for the calculation of thermoelectric properties, the Seebeck coefficients of Fe$_2$VAl were calculated based on the DFT, G_0W_0, and GW_0 electronic structures with the BoltzTraP code

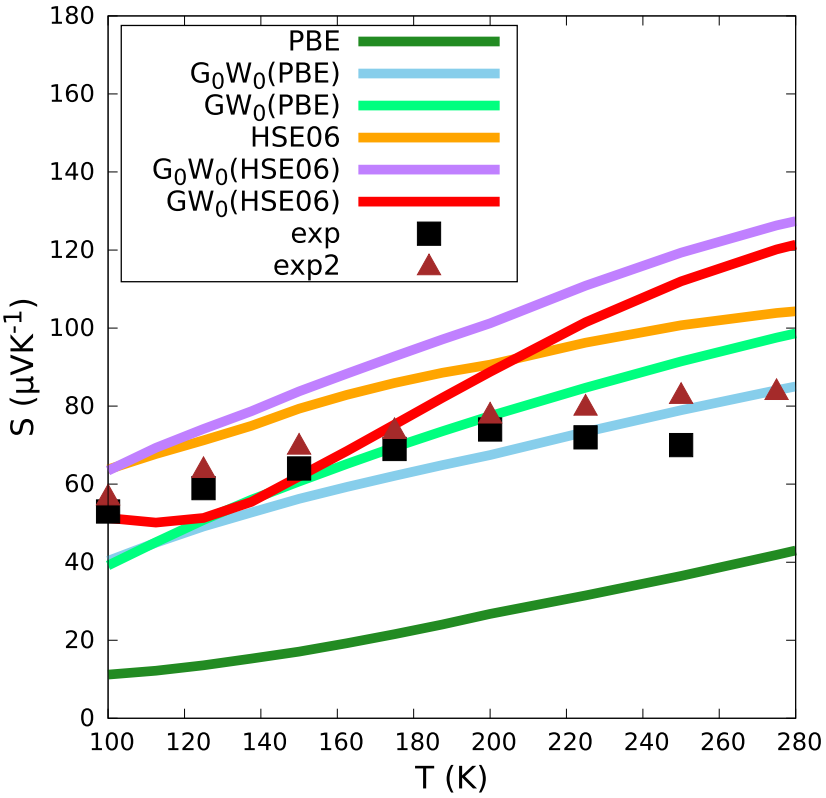

Figure 5. The experimental and calculated Seebeck coefficients (S) as a function of temperatures for Fe_2VAl. The calculated Seebeck coefficients are obtained based on the DFT, G_0W_0, and GW_0 electronic structures for both PBE and HSE06 XC functionals. The black squares (exp) and brown triangles (exp2) are the experimental data from the [45] and [52], respectively.

[55] using rigid-band and constant-relaxation-time approximations. In figure 5, we show the calculated Seebeck coefficients at different temperatures with temperature-dependent carrier concentrations obtained from the experimental hall resistances (R_H) [56] by using the Drude free-electron model ($R_H = 1/ne$ where n is the carrier concentration and e is the elementary charge). It is clear that the Seebeck coefficients obtained from the G_0W_0(PBE) and GW_0(PBE) corrected band structures concur with the experimental values [50, 57]. For HSE06, the GW_0(HSE06) Seebeck coefficients are consistent with the experimental data, especially below 200 K. Although the DFT(HSE06) Seebeck coefficient are relative close to experiment results than the DFT(PBE) ones, which are only half of experimental measurements, the DFT(HSE06) calculated band gap (1.198 eV) does not agree with the experimental values of 0.21–0.28 [14] and 0.10 eV [15]. These results indicate that the *GW* approximations including the many-body corrections are necessary for a better prediction of the band structures and Seebeck coefficients. More details about the calculations of the Seebeck coefficients can be found in the supplemental material (stacks.iop.org/JPhysCM/32/175501/mmedia).

Conclusion

The electronic structures of Fe-based and Ru-based full Heusler compounds have been systematically studied by DFT and *GW* calculations with PBE, PBE + U, and HSE06 XC functionals. Through the analysis of the ADEs, it clearly reveals that the PBE, PBE + U, and HSE06 XC functionals will result in discrepant band structures at the DFT level. The discrepancies are dramatically reduced and get more consistent band structures at the *GW* levels. Moreover, for Fe_2VAl, we have shown that after applying the many-body *GW* corrections, the calculated band gaps and the Seebeck coefficients have a better agreement with the experimental results. Conclusively, to sum up all the results, performing G_0W_0 approximation with PBE starting wavefunctions would be a good strategy to efficiently calculate the accurate band structures of these Heusler compounds. Then, more accurate thermoelectric properties would be obtained based on these corrected electronic structures.

Acknowledgment

The work was supported by the Ministry of Science and Technology, Taiwan, under Grant No. MOST 102-2112-M-001-023-MY3, MOST 105-2112-M-001-007-MY3 (HWL, CRH, and CMW) and MOST 107-2112-M-259-004 (CMC). Computing resources from the Academia Sinica Computing Center of Taiwan are acknowledged.

ORCID iDs

Chun-Ming Chang https://orcid.org/0000-0001-7141-1630

References

[1] Tan G, Zhao L D and Kanatzidis M G 2016 *Chem. Rev.* **116** 12123–49
[2] Graf T, Felser C and Parkin S S P 2011 *Prog. Solid State Chem.* **39** 1–50
[3] Hohenberg P and Kohn W 1964 *Phys. Rev.* **136** B864–71
[4] Kohn W and Sham L J 1965 *Phys. Rev.* **140** A1133–8
[5] Bilc D I, Hautier G, Waroquiers D, Rignanese G M and Ghosez P 2015 *Phys. Rev. Lett.* **114** 136601
[6] Bilc D I and Ghosez P 2011 *Phys. Rev.* B **83** 205204
[7] Do D, Lee M S and Mahanti S D 2011 *Phys. Rev.* B **84** 125104
[8] Bandaru S, Katre A, Carrete J, Mingo N and Jund P 2017 *Nanoscale Microscale Thermophys. Eng.* **21** 237–46
[9] Perdew J P and Levy M 1983 *Phys. Rev. Lett.* **51** 1884
[10] Perdew J P *et al* 2017 *Proc. Natl Acad. Sci. USA* **114** 2801
[11] Singh D J and Mazin I I 1998 *Phys. Rev.* B **57** 14352–6
[12] Guo G Y, Botton G A and Nishino Y 1998 *J. Phys.: Condens. Matter* **10** L119
[13] Weht R and Pickett W E 1998 *Phys. Rev.* B **58** 6855–61
[14] Lue C S and Ross J H 1998 *Phys. Rev.* B **58** 9763–6
[15] Okamura H *et al* 2000 *Phys. Rev. Lett.* **84** 3674–7
[16] Buffon M L C, Laurita G, Lamontagne L, Levin E E, Mooraj S, Lloyd D L, White N, Pollock T M and Seshadri R 2017 *J. Phys.: Condens. Matter* **29** 405702
[17] Wei P C, Huang T S, Lin S W, Guo G Y and Chen Y Y 2015 *J. Appl. Phys.* **118** 165102
[18] Hybertsen M S and Louie S G 1986 *Phys. Rev.* B **34** 5390–413
[19] Godby R W, Schlüter M and Sham L J 1988 *Phys. Rev.* B **37** 10159–75
[20] Faleev S V, van Schilfgaarde M and Kotani T 2004 *Phys. Rev. Lett.* **93** 126406
[21] Shih B C, Xue Y, Zhang P, Cohen M L and Louie S G 2010 *Phys. Rev. Lett.* **105** 146401
[22] Kang W and Hybertsen M S 2010 *Phys. Rev.* B **82** 085203
[23] van Schilfgaarde M, Kotani T and Faleev S 2006 *Phys. Rev. Lett.* **96** 226402
[24] Marini A, Onida G and Del Sole R 2001 *Phys. Rev. Lett.* **88** 016403
[25] Rangel T, Kecik D, Trevisanutto P E, Rignanese G M, Van Swygenhoven H and Olevano V 2012 *Phys. Rev.* B **86** 125125
[26] Meinert M, Friedrich C, Reiss G and Blügel S 2012 *Phys. Rev.* B **86** 245115
[27] Tas M, Şaşığlu E, Galanakis I, Friedrich C and Blügel S 2016 *Phys. Rev.* B **93** 195155
[28] Perdew J P, Burke K and Ernzerhof M 1996 *Phys. Rev. Lett.* **77** 3865–8
[29] Perdew J P, Ernzerhof M and Burke K 1996 *J. Chem. Phys.* **105** 9982–5
[30] Ernzerhof M and Scuseria G E 1999 *J. Chem. Phys.* **110** 5029–36
[31] Kuo C N, Lee H W, Wei C M, Lin Y H, Kuo Y K and Lue C S 2016 *Phys. Rev.* B **94** 205116
[32] Heyd J, Scuseria G E and Ernzerhof M 2003 *J. Chem. Phys.* **118** 8207
[33] Krukau A V, Vydrov O A, Izmaylov A F and Scuseria G E 2006 *J. Chem. Phys.* **125** 224106
[34] Tseng C W, Kuo C N, Lee H W, Chen K F, Huang R C, Wei C M, Kuo Y K and Lue C S 2017 *Phys. Rev.* B **96** 125106
[35] Galanakis I, Dederichs P H and Papanikolaou N 2002 *Phys. Rev.* B **66** 174429
[36] Chou J P, Chen H Y T, Hsing C R, Chang C M, Cheng C and Wei C M 2009 *Phys. Rev.* B **80** 165412
[37] Kresse G and Furthmüller J 1996 *Comput. Mater. Sci.* **6** 15–50
[38] Kresse G and Furthmüller J 1996 *Phys. Rev.* B **54** 11169–86
[39] Kresse G and Joubert D 1999 *Phys. Rev.* B **59** 1758–75
[40] Shishkin M and Kresse G 2007 *Phys. Rev.* B **75** 235102
[41] Shishkin M and Kresse G 2006 *Phys. Rev.* B **74** 035101
[42] Blöchl P E 1994 *Phys. Rev.* B **50** 17953–79
[43] Henderson T M, Scalmani G, Izmaylov A F and Scuseria G E 2009 *J. Chem. Phys.* **131** 044108
[44] Garza A J and Scuseria G E 2016 *J. Phys. Chem. Lett.* **7** 4165–70
[45] Anisimov V I and Gunnarsson O 1991 *Phys. Rev.* B **43** 7570–4
[46] Monkhorst H J and Pack J D 1976 *Phys. Rev.* B **13** 5188–92
[47] Murnaghan F D 1944 *Proc. Natl Acad. Sci. USA* **30** 244
[48] Hamann D R and Vanderbilt D 2009 *Phys. Rev.* B **79** 045109
[49] Mostofi A A, Yates J R, Pizzi G, Lee Y S, Souza I, Vanderbilt D and Marzari N 2014 *Comput. Phys. Commun.* **185** 2309–10
[50] Knapp I, Budinska B, Milosavljevic D, Heinrich P, Khmelevskyi S, Moser R, Podloucky R, Prenninger P and Bauer E 2017 *Phys. Rev.* B **96** 045204
[51] Lue C S and Ross J H 2001 *Phys. Rev.* B **63** 054420
[52] Ramachandran B, Lin Y, Kuo Y, Kuo C, Gippius A and Lue C 2018 *Intermetallics* **92** 36–41
[53] Mondal S, Mazumdar C and Ranganathan R 2013 *AIP Conf. Proc.* **1512** 978–9
[54] Cerba P, Vilasi M, Malaman B and Steinmetz J 1993 *J. Alloys Compd.* **201** 57–60
[55] Madsen G K and Singh D J 2006 *Comput. Phys. Commun.* **175** 67–71
[56] Nishino Y 2000 *Intermetallics* **8** 1233–41
[57] Skoug E J, Zhou C, Pei Y and Morelli D T 2009 *J. Electron. Mater.* **38** 1221–3